The Formation of Veins in Greenschist Facies Rocks and the Early Deformation of the Meguma Group, Eastern Nova Scotia

B.H. O'Brien

Department of
Mines and Energy

contribution to
Canada – Nova Scotia
Co-operative Mineral Program
1981-84

86-01936/

Nova Scotia
Department of
Mines and Energy

Paper 85-2

The Formation of Veins in Greenschist Facies Rocks and the Early Deformation of the Meguma Group, Eastern Nova Scotia

by

B.H. O'Brien

Honourable Joel R. Matheson, Q.C., Minister
John J. Laffin, P.Eng., FEIC, Deputy Minister

HALIFAX, NOVA SCOTIA

1985

TABLE OF CONTENTS

Abstract 1
Introduction 1
The Syntectonic D_s Veins 2
Field Appearance 2
Microscopic Appearance 4
Nature of the Platelets 10
Syn-D_s Side Veins 13
Wall Rock Inclusions 18
Honeycomb Structure 21
Textures Indicative of Platelet-parallel Slip 21
Summary of Syn-D_s Veins 23
Models for the Origin of Syntectonic D_s Veins 26
Model 1: Burial with Incipient Layer-parallel Shortening 28
Model 2: Layer-parallel Shear 28
Acknowledgments 31
References 33

LIST OF FIGURES

Figure 1. Map showing the locations where veins were examined in detail 1
Figure 2. Thin, syn-D_s vein crosses from the stratigraphic base to the stratigraphic top of a crosslaminated sandstone 3
Figure 3. Bifurcation of thin, syn-D_s vein within laminated sandstone 3
Figure 4. Syn-D_s vein illustrating characteristic laminations 4
Figure 5a. Top view of a preferentially eroded, syn-D_s laminated vein. Within the vein, light coloured quartz veinlets occur in dark coloured carbonate. In the bottom left of the photograph two orientations of veinlets are observable 5
Figure 5b. Cross-section of subhorizontal syn-D_s vein composed of dark coloured calcite with light coloured subvertical quartz veinlets 5
Figure 6. Schematic block diagram of a principal, syn-D_s vein illustrating the relationship between platelets and veinlets 6
Figure 7. Two quartz veinlets terminate against a quartz platelet interlayered with carbonate platelets. Crossed nicols 6
Figure 8a. Grooved lineations on the surface of quartz platelets in a syn-D_s vein 7
Figure 8b. Grooved lineations folded around the hinges of F_g minor folds 7
Figure 9. Well developed platelets in a syn-D_s vein near a wall rock inclusion. The inclusion is veined by quartz from the platelets. Crossed nicols 8
Figure 10. Planar bands of white micas separating optically continuous quartz platelets that are optically continuous with one another. Crossed nicols 8

Figure 11. A thin band of white micas in a laminated, syn-D_s vein splits into four bands, each separated by optically continuous quartz. Crossed nicols 9

Figure 12. Planar band of material separating two quartz platelets dips from the top right to the bottom left of the photograph. The quartzofeldspathic material illustrates inequant grain boundaries, and the micas are thin and flakey. Crossed nicols 9

Figure 13. Intraplatelet micaceous bands dipping consistently in one direction in a laminated, syn-D_s vein. These bands display an 'imbricate' relationship with the planar micaceous bands sited along the platelet surfaces. Crossed nicols 10

Figure 14. Low angle, intraplatelet micaceous bands terminating within a quartz platelet. Crossed nicols 11

Figure 15. High angle, intraplatelet micaceous bands occurring as curved surfaces resembling 'foresets' or 'imbricates'. Crossed nicols 11

Figure 16a. Material comprising the intraplatelet bands in a cross-laminated, syn-D_s vein appears to be preferentially derived from one side of an included rock fragment. Crossed nicols 12

Figure 16b. Angular wall rock inclusion within a principal syn-D_s vein. Platelets and inclusion bands lie parallel to the margin of the principal vein 12

Figure 17a. Light coloured, unstrained, single crystal of quartz occurs along a surface separating calcite platelets. Elsewhere in the photograph this surface is marked by the (0001) calcite glide twin. Crossed nicols 14

Figure 17b. Single crystal of quartz extends from the serrated margin of a subvertical veinlet approximately 0.2 mm and locally separates two calcite platelets. Crossed nicols 14

Figure 18. Cross-section of a layered sequence of calcite platelets with the (0001) and the (0112) glide twins indicated ... 15

Figure 19a. Syn-D_s principal vein with side vein or offshoot emplaced into hanging wall 15

Figure 19b. Tightly folded side veins or offshoots in the footwall of a laminated, syn-D_s principal vein. Crossed nicols 15

Figure 20. Side veins of quartz optically continuous with the basal quartz platelet of the principal vein, extend downwards into the footwall metasediment. (A) the geometric relationships among the side veins, the S_s cleavage, the F_s folds, the principal vein and the bedding (S_o); (B) the geometric relationships among the side veins, the S_s cleavage, the F_s folds, the principal vein and the inclusion bands 16

Figure 21. Subvertical side veins extending downward from the basal platelet of a laminated, principal vein into the footwall metasediment. Note the included material within the quartz veins and the strong cleavage in the host strata subparallel to the basal platelet. Crossed nicols 16

Figure 22. Cross-section of subvertical side vein in footwall metasediment displaying inclusion bands arranged parallel to the veinlet margin. The quartz forming this part of the vein is an optically continuous, single crystal. Crossed nicols 17
Figure 23. Cross-section of a single crystal side vein in cleaved host rock 17
Figure 24. Subrecumbent F_S microfolds fold subvertical veinlets and the single quartz crystals so that they begin to develop subgrains. Note the axial planar S_S cleavage in the host strata. Crossed nicols 18
Figure 25. Wall rock inclusions are spatially related to micaceous bands separating the platelets in the laminated, syn-D_S veins. Crossed nicols 19
Figure 26. The included rock fragment in the top left of the photograph carries the same cleavage as the wall rock at the bottom right. The micaceous bands separating the variably recrystallized quartz platelets also contain micas with the same preferred orientation. Crossed nicols 19
Figure 27a. A single crystal veinlet with traces of inclusion bands is emplaced into a rock fragment parallel to the laminations of a principal, syn-D_S vein. Crossed nicols 20
Figure 27b. Included rock fragment containing two veinlets (one with locally developed inclusion bands) normal to the laminations in the principal vein. The veinlets emanate from single crystal platelets shown at bottom of the photograph. Crossed nicols 20
Figure 28. Serrated margin of a fibrous quartz veinlet within calcite platelets. Crossed nicols 22
Figure 29. Subvertical inclusion bands in a quartz veinlet in a laminated, syn-D_S vein. The inclusion bands are composed of fragments of calcite. Crossed nicols 22
Figure 30. Inclusion trails defined by calcite grains in a subvertical quartz veinlet. Crossed nicols 24
Figure 31. Displacement surfaces, within micaceous bands at platelet boundaries, pass through included rock fragments. Crossed nicols 24
Figure 32. Recrystallized veinlets deformed by open folds below a displacement surface parallel to the platelets and inclusion bands in a laminated, syn-D_S vein. Crossed nicols 25
Figure 33. An e-lamellae (0112) twin in a calcite platelet is displaced along a (0001) glide twin. Crossed nicols 25
Figure 34a. Dendritic chlorite enclosed 'poikilitically' in a single crystal of quartz. The latter comprises a platelet in a laminated, quartz-carbonate vein. Crossed nicols 27
Figure 34b. Vermicular, fibrous growths of chlorite set in optically continuous quartz. Crossed nicols 27

Figure 35. Models depicting the stress orientations for tensile fractures formed during compaction and diagenesis. (A) portrays the concomitant development of vertical veinlets and a horizontal compaction fabric in flat strata affected by a vertical maximum principal stress; (B) shows the opening of the horizontal platelets in flat strata carrying a bedding-parallel compaction fabric. Here the maximum principal stress is applied in the horizontal plane 29

Figure 36. Models depicting the stress orientations for shear and tensile fractures formed during D_s layer-parallel shear. (A), (B) and (C) are cross-sections of a horizontal bed with the bedding planes acting as shear planes. The maximum principal stress is drawn with a constant orientation with respect to bedding and the principal shear planes in (A), (B) and (C) 30

THE FORMATION OF VEINS IN GREENSCHIST FACIES ROCKS AND THE EARLY DEFORMATION OF THE MEGUMA GROUP, EASTERN NOVA SCOTIA

B. E. O'Brien

ABSTRACT

Stratabound principal veins displaying lamination or honeycomb structure form the earliest group of syntectonic veins in the Meguma Group of eastern Nova Scotia. Textures related to the growth or dilation history of these veins include optically continuous crystal platelets, margin-parallel inclusion bands, fibrous or serrated veinlets, offshoots with trails of preferentially oriented phyllosilicates and pull-apart inclusions of cleaved wall rock. Folding and attenuation, lineation, recrystallization and twinning are products of postemplacement deformation of the veins. The stratabound veins are interpreted to have opened in the flat-lying metasediments while the oldest host rock foliation (S_0) was developing.

INTRODUCTION

Auriferous vein arrays of variable composition and morphology were studied in selected areas of southwestern Guysborough County, eastern Nova Scotia (Fig. 1). The arrays are hosted by Meguma Group metasedimentary

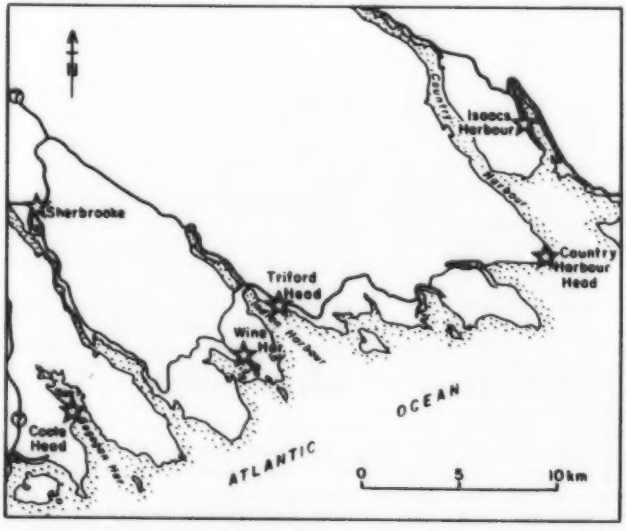

Figure 1. Map showing the locations where veins were examined in detail.

rocks in the chlorite and biotite zones of regional metamorphism. The host rocks were deformed by the D_S, D_T and D_C episodes of regional deformation (O'Brien, 1983a), each of which produced cleavage, folding and lineation. Veins formed sporadically throughout, as well as after, these deformation episodes. In many places, the veins have locally altered the metasediments (Smith, 1983; Haynes, 1983).

Syntectonic vein-filled fractures formed (1) prior to folding of the flat-lying strata, (2) during the development of the major folds and (3) during the development of the major faults. This paper deals exclusively with the first group of veins.

THE SYNTECTONIC D_S VEINS

Field Appearance

Syn-D_S veins occur within rocks of the Goldenville Formation throughout southwestern Guysborough County. Within the established gold districts the veins are referred to as 'leads'. Syn-D_S veins were not observed locally in rocks of the Halifax Formation but this may be a function of its limited outcrop and poor exposure. In any cross-section of Goldenville strata, syn-D_S veins are nested in certain stratigraphic horizons. In parallel sections along strike, however, the veins are commonly observed to be either (1) absent from a correlative horizon defined with respect to the base of the Halifax Formation, or (2) are present but nested at a stratigraphic level well above, or below, those of other sections.

Concordant syn-D_S veins are most common and thickest in shales. However, thin, closely stacked, laterally continuous veins are found in sandstones. Near the top of graded beds, in particular, syn-D_S veins are seen in spatial association with well developed S_S cleavage.

In several places, syn-D_S veins exhibit a low angle discordant relationship to bedding. For example, some of the thinnest syn-D_S veins are seen to cross from the stratigraphic base to the stratigraphic top of single, 5-15 mm thick, crosslaminated units (Fig. 2). Others which appear to lie at specific horizons within certain parallel laminated units are observed to bifurcate before coalescing to form a single vein (Fig. 3). In doing so, they include fragments of laminated host rock. Postemplacement deformation of syn-D_S veins makes the intersection angle between bedding laminations and vein margins smaller. No amount of deformation would make an original bedding-parallel contact appear to be discordant and stratigraphically transgressive.

Syn-D_S veins are composed predominantly of quartz and calcite with white mica, chlorite, rock inclusions and variable amounts of sulphides. In the field and in hand specimen, these veins are characteristically laminated (Fig. 4). Quartz and calcite have a distinct shape in the stratabound laminated veins, occurring as parallel platelets commonly 1-3 mm thick. Each platelet is separated by a thin band of darker coloured material. The length to thickness ratio of some platelets exceeds 100:1. The platelets are parallel to the sides of the veins, but not necessarily to the bedding in the host rocks. In places, discontinuous, platelet-

Figure 2. Thin, syn-D_8 vein (arrows) crosses from the stratigraphic base (left hand side) to the stratigraphic top (right hand side) of a crosslaminated sandstone. The hand lens is 3 cm long.

Figure 3. Bifurcation of thin, syn-D_8 vein within laminated sandstone. Arrow indicates position of vein split. Field of view is 12 cm x 8 cm.

parallel, dark coloured bands form 'columnar' structures (cf. Haynes, 1983) that extend from the footwall or hangingwall into the vein at various angles. However, not every syn-D_8 vein is laminated. Where primary vein textures are not affected by recrystallization, it is evident that massive or drusy quartz and calcite pass into areas of quartz and calcite platelets.

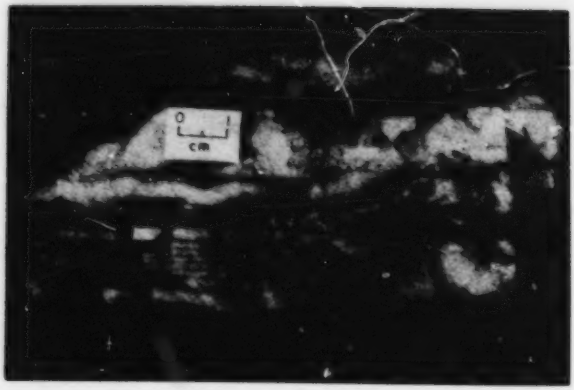

Figure 4. Syn-D_g vein illustrating characteristic laminations.

Three dimensional 'honeycomb' structure (Fig. 5a and b) is common in laminated veins. Two sets of veinlets, within and normal to the principal vein, intersect in the plane of the platelets to define rhombs and parallelograms (Fig. 6). In some cross-sections these veinlets rise through a sequence of platelets. In other sections they terminate abruptly against or pass laterally into a platelet (Fig. 7). In doing so they create a discontinuous three dimensional 'honeycomb' structure (Fig. 6). Commonly, the veinlets are composed of a different mineral species than the platelets.

In the field, syn-D_g veins display lineations that are fibrous and have topography (Fig. 8a and b). The lineations occur on the surface of individual platelets. In some localities the pitch of the lineations on successive platelets is constant throughout the vein, and in others it varies systematically presumably indicating changing kinematic conditions. In places, where the laminated veins are locally folded by minor F_g folds, the lineations make variable angles with the F_g fold hinges.

Syn-D_g veins possessing platelets, veinlets and side veins are folded by minor F_g folds (O'Brien, 1983a) and steepened to various attitudes as a result of large-scale F_g folding. Their original geometric relationships are best preserved near the hinges of gently plunging, major folds.

Microscopic Appearance

Thin sections of the syn-D_g laminated veins illustrate the nature of the platelets and the relationship between the platelets and the dark coloured material separating them. Veins spared from recrystallization show individual platelets composed of single tabular crystals of quartz and, less commonly, calcite. Each platelet is in optical continuity with its neighbours despite the presence of intervening dark coloured

Figure 5a. Top view of a preferentially eroded, syn-D_3 laminated vein. Within the vein, light coloured quartz veinlets occur in dark coloured carbonate. In the bottom left of the photograph two orientations of veinlets are observable. The field of view is 35 cm x 25 cm.

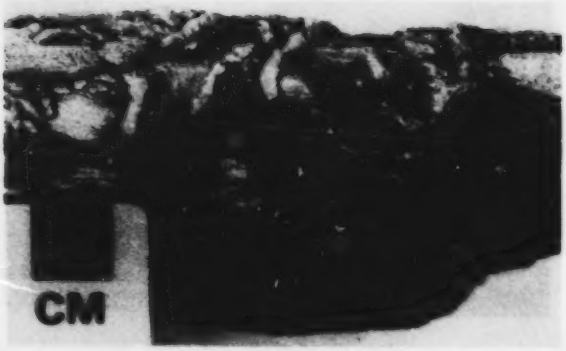

Figure 5b. Cross-section of subhorizontal syn-D_3 vein composed of dark coloured calcite with light coloured subvertical quartz veinlets. In the extreme left of the photograph the veinlets are seen to be confined to the area between the footwall and the hanging wall of the main vein.

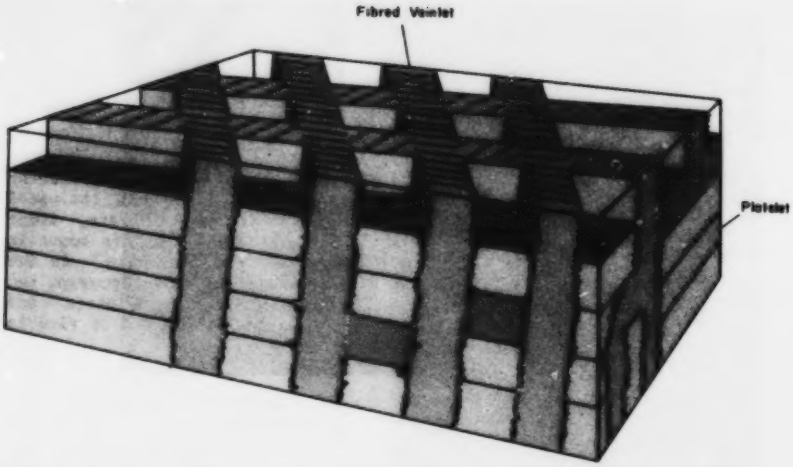

Figure 6. Schematic block diagram of a principal, syn-D_s vein illustrating the relationship between platelets and veinlets.

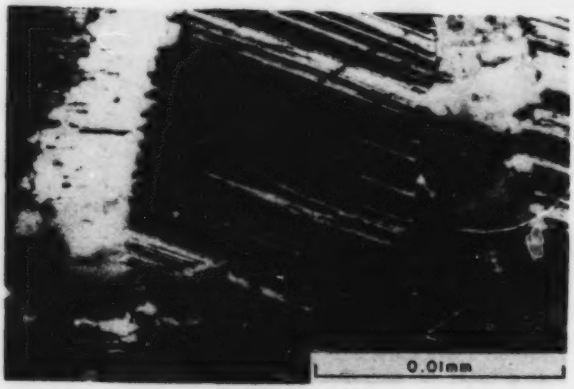

Figure 7. Two quartz veinlets terminate against a quartz platelet interlayered with carbonate platelets. Arrows point to platelet boundaries. Crossed nicols.

Figure 8a. Grooved lineations on the surface of quartz platelets in a syn-D_g vein.

Figure 8b. Grooved lineations folded around the hinges of F_g minor folds.

layers. Within the veins the spacing between the layers is variable and therefore the platelets are of variable thickness at any given point along their length. This variation is best seen approaching rock inclusions, where the platelet thickness and the spacing between dark layers gradually diminishes (Fig. 9).

In the laminated veins, the material separating the platelets is commonly arranged in thin (<0.05 mm), planar bands (Fig. 10). For the most

part, the planar bands are composed of minute white micas or chlorites a few grains thick. The length to thickness ratio of the bands exceeds 50:1. In places, thin mica bands terminate laterally within a single platelet. The bands split or fork into a series of isolated grains separated by optically continuous quartz (Fig. 11). The micaceous bands also thicken laterally and where the bands thicken to 0.05-0.10 mm, they are comprised of quartz and feldspar in addition to the white mica (Fig. 12).

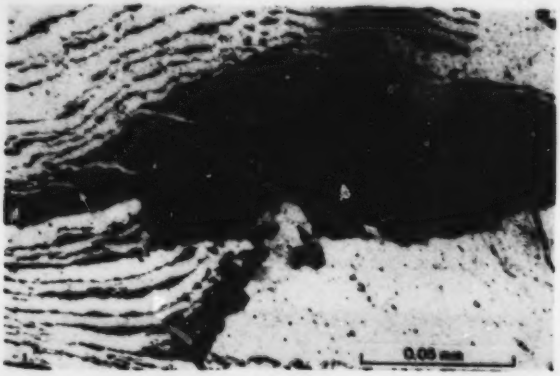

Figure 9. Well developed platelets in a syn-D_3 vein near a wall rock inclusion. The inclusion is veined by quartz from the platelets. The dark coloured material separating the platelets is the same as that comprising the rock fragment. Arrow points to a single crystal vein crossing the fragment and joining one platelet to another. Crossed nicols.

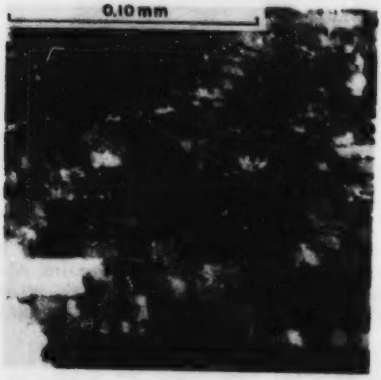

Figure 10. Planar bands of white micas (see arrow) separating optically continuous quartz platelets that are optically continuous with one another. Crossed nicols.

Figure 11. A thin band of white micas in a laminated, syn-D_s vein splits into four bands, each separated by optically continuous quartz. See arrows in the centre of photograph. Crossed nicols.

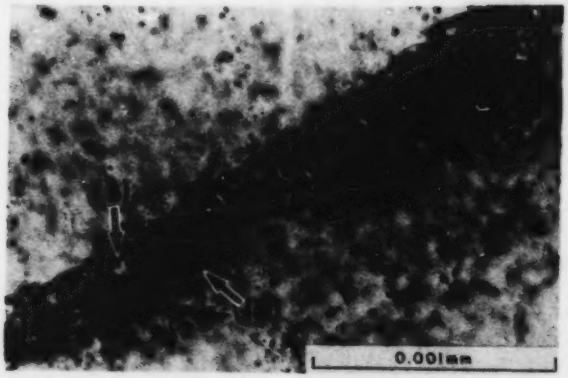

Figure 12. Planar band of material separating two quartz platelets dips from the top right to the bottom left of the photograph. The quartzofeldspathic material (arrow A) illustrates inequant grain boundaries, and the micas (arrow B) are thin and flakey. Crossed nicols.

Some laminated veins contain micas within platelets as well as along their surfaces. The intraplatelet micas show a preferred orientation. They occur in a parallel series of straight, curved or sinuous planes and commonly merge with the planar bands separating the platelets in an 'imbricate' fashion. 'Crosslamination' of this type has been recorded from slickensided quartz-carbonate veins in the Alberta coalfields (Morris and Barron, 1968). In multiplatelet veins the dip direction of the 'foresets' is generally consistent from platelet to platelet (Fig. 13). The 'foresets' are of two types: (1) a low angle variety extending from the planar 'topset' as a slightly curved plane and terminating within the platelet (Fig. 14) and (2) a high angle variety extending from the planar 'topset' to the planar 'bottomset' as a curved or sinuous plane (Fig. 15). Both types are chiefly defined by grains of white mica set in optically continuous, single crystals of quartz. The grains comprising the 'foresets' seem to be preferentially derived from particular sides of angular rock fragments (Fig. 16a), while those forming the 'topsets' and 'bottomsets' appear to originate from opposing sides of the same inclusions (Fig. 16b).

Nature of the Platelets

In thin sections of unrecrystallized parts of syn-D_s laminated veins, grain boundaries are rarely observed within platelets. Where present, however, they form variable though generally high angles with the

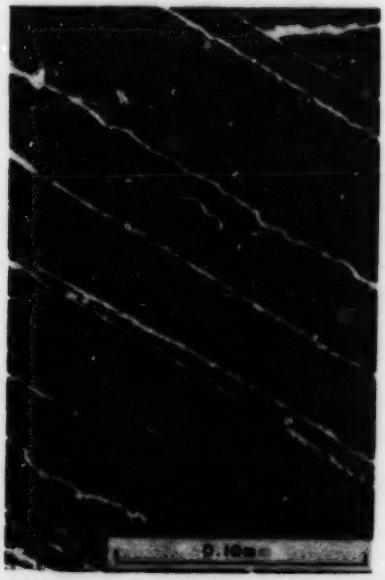

Figure 13. Intraplatelet micaceous bands dipping consistently in one direction in a laminated, syn-D_s vein. These bands display an 'imbricate' relationship with the planar micaceous bands sited along the platelet surfaces. Crossed nicols.

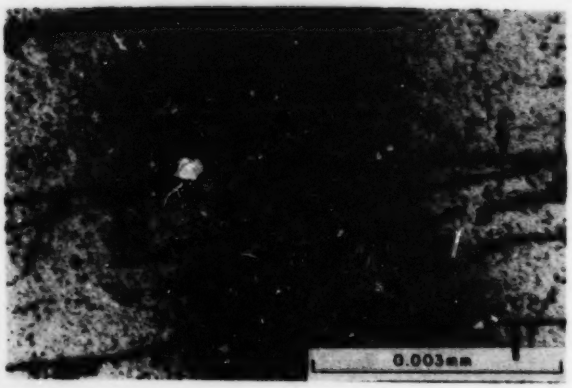

Figure 14. Low angle, intrapletelet micaceous bands terminating within a quartz platelet. Arrows point to the boundaries of the platelet and the platelet-parallel micaceous bands. Crossed nicols.

Figure 15. High angle, intraplatelet micaceous bands occurring as curved surfaces resembling 'foresets' or 'imbricates'. Crossed nicols.

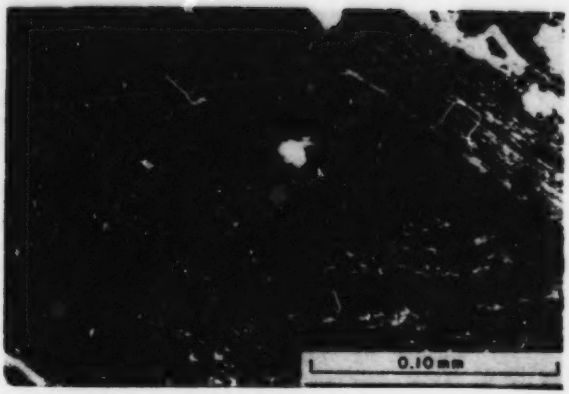

Figure 16a. Material comprising the intraplatelet bands in a cross-laminated, syn-D_s vein appears to be preferentially derived from one side of an included rock fragment. Crossed nicols.

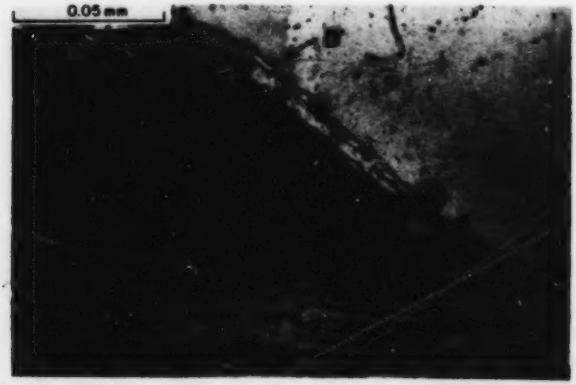

Figure 16b. Angular wall rock inclusion within a principal syn-D_s vein. Platelets and inclusion bands lying parallel to the margin of the principal vein are shown by arrow marked (A). Inclusion bands and platelets dipping from top centre to bottom right (arrow marked B) are derived from an opposite side of the same inclusion.

platelet boundaries. C-axes of quartz and calcite, in sections cut perpendicular to the laminations and the vein wall, show preferred orientations. C-axes measurements are constant for at least several centimetres along a

single platelet or across a succession of platelets. However, the C-axis orientation that is preferred varies from vein to vein or from one part of a laminated vein to another. Vein crystals of quartz and calcite are, therefore, quite large and randomly oriented with respect to the margin-parallel laminations. Cross-sections of calcite platelets in thin section show two, well developed, polysynthetic glide twins (Fig. 17a and 17b), the e-lamellae twinned on (0112) and another less common lamellar twin on (0001) (Fig. 18). The (0001) twin is coincident with the surface of the calcite platelets in many of the laminated veins. Similar textures have been described in laminated veins from Silurian slates in North Wales (Nicholson, 1966). The tabular form of the platelets does not reflect the habit of the trigonal quartz and calcite crystals.

Syn-D_s Side Veins

Side veins or offshoots from the principal syn-D_s veins (Fig. 19a and b) occur both in the hangingwall and the footwall. They show branch fractures and asymmetrically forked terminations (Beach, 1980). This suggests that the hangingwall and footwall were competent and had a finite tensile or shear strength at the time the syn-D_s side veins were emplaced.

The primary textures of the small side veins are rarely seen. This is because most side veins have been steepened with the principal veins becoming tightly crenulated by F_g and extensively recrystallized. Concordant syn-D_s veins near the hinges of some of the major folds, however, have side veins which still bear evidence of their original relationships to the subhorizontal footwall and hangingwall. In several localities, subvertical side veins extend downward, approximately 4-8 mm, from the basal platelet of a subhorizontal laminated vein into a footwall of right-way-up, laminated shale or wacke (Figs. 20 and 21). Many of the side veins bifurcate and link laterally with other side veins. Subvertical S_g slaty cleavage is almost perpendicular to the principal vein, but it is subparallel to the side veins. Weak upright F_g crenulations fold the principal vein. In the footwall these crenulations affect the veins which link the subvertical side veins (Fig. 20).

The syn-D_s side veins have growth textures which are similar to the principal veins. Where the basal platelet of the principal vein is quartz, the subvertical side vein extending from the principal vein is also quartz. The quartz comprising the side vein is an optically continuous, single crystal which passes without interruption into the subhorizontal basal platelet. Thin side veins commonly display a subvertical median suture. The thicker ones illustrate a series of subvertical mica-rich bands, all of which are parallel to the vein margin (Figs. 20 and 22). The bands are composed of the same material as the footwall and herein they are referred to as inclusion bands.

Thin sections show that the inclusion bands are mostly made up of white micas. The micas form trails orientated nearly perpendicular to the vein margin and the inclusion bands (Fig. 23). These inclusion trails lie in approximately the same plane as the micas which define the external S_s cleavage in the footwall (O'Brien, 1983a). S_s lies subparallel to the principal vein and the bedding, but almost at right angles to the

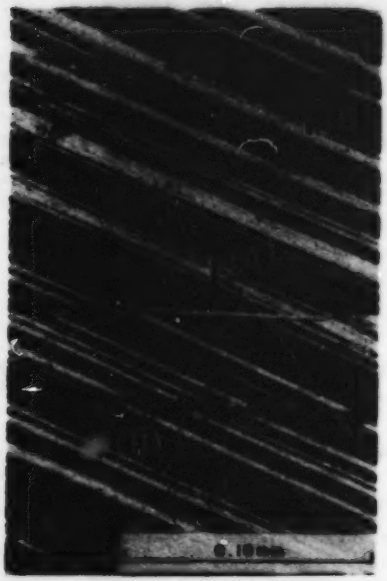

Figure 17a. Light coloured, unstrained, single crystal of quartz (arrow A) occurs along a surface separating calcite platelets. Elsewhere in the photograph this surface is marked by the (0001) calcite glide twin (arrow B). Crossed nicols.

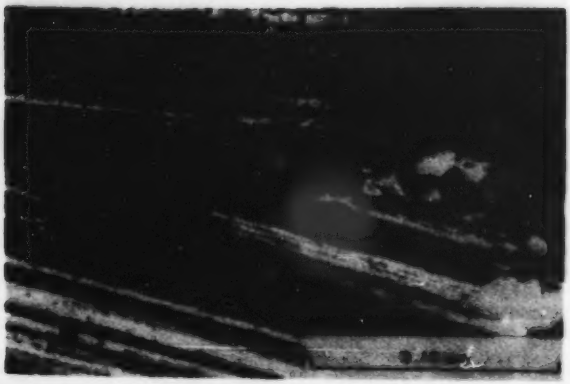

Figure 17b. Single crystal of quartz extends from the serrated margin of a subvertical veinlet approximately 0.2 mm and locally separates two calcite platelets. Crossed nicols.

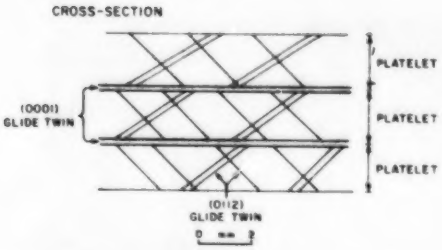

Figure 18.
Cross-section of a layered sequence of calcite platelets with the (0001) and the (0112) glide twins indicated.

Figure 19a.
Syn-D_3 principal vein with side vein or offshoot emplaced into hanging wall. The pencil is 10 cm long.

Figure 19b.
Tightly folded side veins or offshoots in the footwall of a subhorizontal laminated, syn-D_3 principal vein. Crossed nicols.

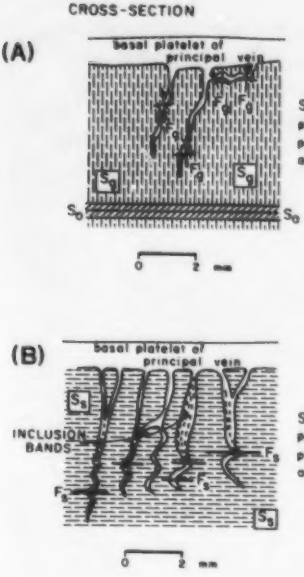

Figure 20. Side veins of quartz optically continuous with the basal quartz platelet of the principal vein, extend downwards into the footwall metasediment. (A) the geometric relationships among the side veins, the S_g cleavage, the F_g folds, the principal vein and the bedding (S_0); (B) the geometric relationships among the side veins, the S_s cleavage, the F_s folds, the principal vein and the inclusion bands.

Figure 21. Subvertical side veins extending downward from the basal platelet of a laminated, principal vein into the footwall metasediment. Note the included material within the quartz veins (arrow A) and the strong cleavage in the host strata subparallel to the basal platelet (arrow B). Crossed nicols.

Figure 22. Cross-section of subvertical side vein in footwall metasediment displaying inclusion bands (arrow A) arranged parallel to the veinlet margin (arrow B). The quartz forming this part of the vein is an optically continuous, single crystal. Crossed nicols.

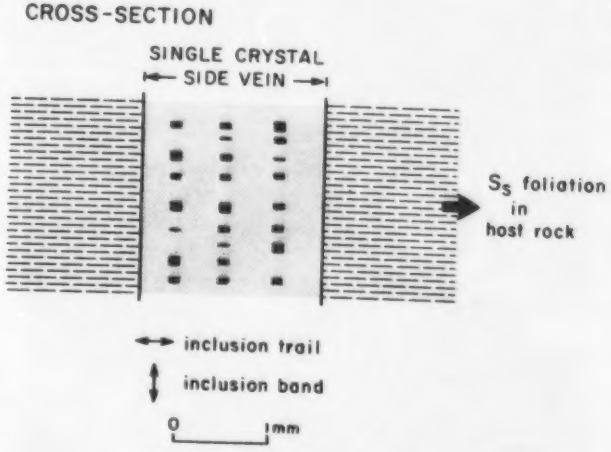

Figure 23. Cross-section of a single crystal side vein in cleaved host rock. Note the orientation of the phyllosilicates defining inclusion bands and inclusion trails in the side vein and note the S_s foliation orientation in the host rock.

subvertical side veins. The S_d cleavage in the footwall is axial planar to subrecumbent folds of the side veins. D_g deformation caused recrystallization of the single crystals of quartz near the cores of the F_g folds (Fig. 24). The regional S_g slaty cleavage which is axial planar to upright crenulations of the principal vein locally overprints the S_g cleavage (Fig. 20). It appears that the side veins extending from the principal veins opened to include or occlude S_g micas and that S_g cleavage continued to be produced after the side veins ceased to form. F_g minor folds deform both the principal veins (Fig. 4 in O'Brien, 1983a) and the side veins.

Wall Rock Inclusions

Wall rock inclusions are present in the principal syn-D_g veins. The inclusions are spatially associated with the planar micaceous bands in the laminated portions of these veins (Fig. 25). The inclusions are seen to be penetratively cleaved where they are thick (Fig. 26). The cleavage is subparallel to the inclusion bands, the platelet and the vein margins, and is coincident with the S_g cleavage in the wall rocks. Platelets of quartz and calcite hosting the strongly cleaved fragments are unstrained or locally undeformed. In places, the cleaved inclusions seem to be protected or armoured by large crystals in a 'poikilitic' arrangement.

On approaching the wall rock fragments, inclusion bands become more closely spaced, yet continue to separate platelets of single quartz crystals. Thin sections show the wall rock inclusions veined by quartz in directions parallel and perpendicular to the platelets (Fig. 27a and b). The veinlets in the rock fragments pass continuously into the quartz of the bounding platelets. Inclusion bands are parallel to the margins of the veinlets and the margins of the rock inclusions (Fig. 27b). Where the edge

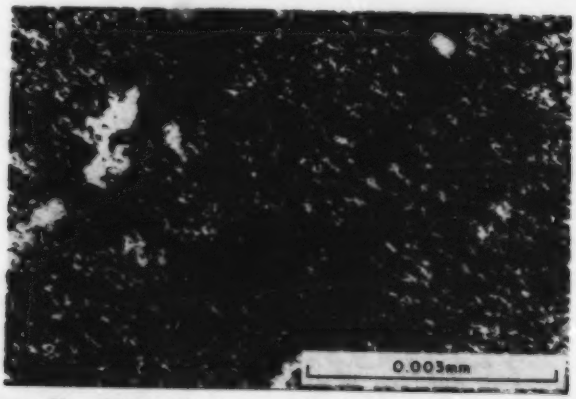

Figure 24. Subrecumbent F_g microfolds fold subvertical veinlets and the single quartz crystals so that they begin to develop subgrains. Note the axial planar S_g cleavage in the host strata. Crossed nicols.

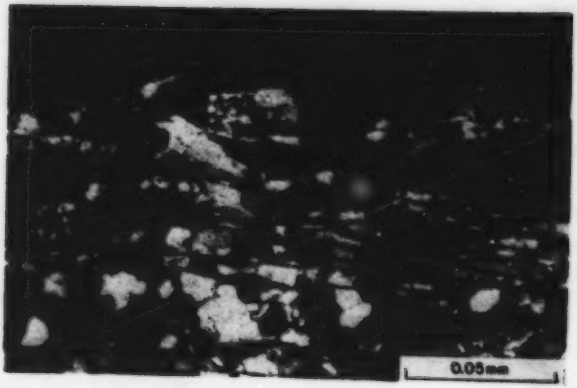

Figure 25. Wall rock inclusions are spatially related to micaceous bands separating the platelets in the laminated, syn-D_s veins. Arrow points to where wall rock inclusion passes laterally into an inclusion band. The hanging wall contact is observable at the top of the photograph. Crossed nicols.

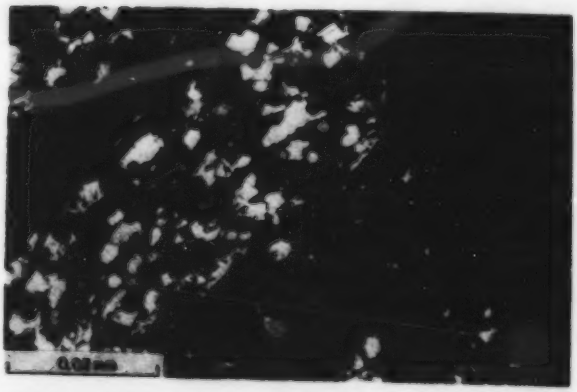

Figure 26. The included rock fragment in the top left of the photograph carries the same cleavage as the wall rock at the bottom right. The micaceous bands separating the variably recrystallized quartz platelets also contain micas with the same preferred orientation. Crossed nicols.

Figure 27a. A single crystal veinlet with traces of inclusion bands (arrow A) is emplaced into a rock fragment parallel to the laminations (arrow B) of a principal, syn-D_3 vein. Crossed nicols.

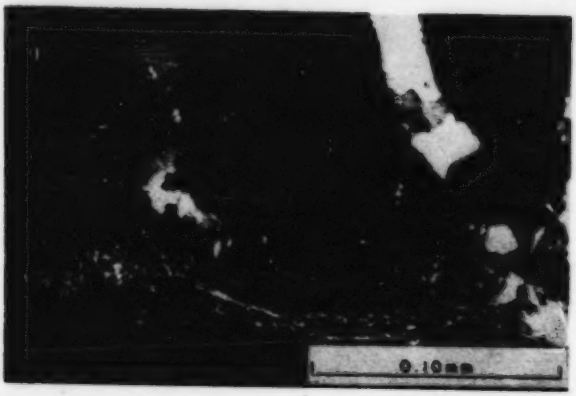

Figure 27b. Included rock fragment containing two veinlets (one with locally developed inclusion bands) normal to the laminations in the principal vein. The veinlets emanate from single crystal platelets shown at bottom of the photograph. Crossed nicols.

of a rock fragment follows the margins of a mutually perpendicular platelet and veinlet, the inclusion bands in the single crystal show the ghost outline of the fragment. It appears that the veinlets open in the inclusion in the same way that the side veins open from the basal platelet into the footwall of the principal vein. In situ or para-autochthonous wall rock fragments seem to pass into the inclusion bands and the quartz veinlets appear to pass laterally and vertically into the platelets. In this way the wall rock inclusions are filled with quartz, dilated, fragmented and intercalated within the main vein.

Honeycomb Structure

The veinlets within the laminated principal veins (Fig. 6) are similar to the veinlets in the rock inclusions and the side veins in the footwall or hangingwall. Although some comprise single quartz crystals, many others are fibrous. The fibres are perpendicular to the serrated margins of the subvertical veinlets (Fig. 28) and lie in a plane parallel to the calcite or quartz platelets. In places, single crystals of quartz up to 0.04 mm thick extend laterally approximately 2.0 mm from a fibrous veinlet onto the surface of a calcite platelet. Here the quartz is interlayered with the tabular calcite crystals (Fig. 17a and b). Elsewhere, the quartz veinlets intruded vertically into the laminated sequence of the platelets.

In some places, subvertical quartz veinlets in the honeycomb structure display excellent inclusion bands and inclusion trails. For the most part, the inclusions are grains of calcite presumably derived from the platelets which the veinlets intruded. In a quartz veinlet 1 mm thick, for example, there are as many as five parallel inclusion bands, each composed of fragments of calcite (Fig. 29). The inclusion trails consist of calcite grains lying parallel to the surface of the platelet and the long axes of the quartz fibres (Fig. 30). Within the syn-Ds laminated veins the subvertical veinlets contain the subhorizontal platelets, whereas in the host rocks the subvertical side veins contain the subhorizontal S_s cleavage.

The honeycomb structure of the principal syn-D_s veins is probably an indicator of the way in which the syntectonic veins were opened. The subhorizontal platelets and margin parallel inclusion bands indicate a vertical extension, and the fibrous subvertical veinlets imply a broadly contemporaneous horizontal extension.

Textures Indicative of Platelet-parallel Slip

Thin sections of the principal syn-D_s veins illustrate textures probably produced by displacement or slip along the platelet surfaces.

(1) In 'crosslaminated' quartz veins the 'topsets' represent margin-parallel inclusion bands, while the 'foreset' inclusions dip more steeply within the platelet. In many specimens, especially those that have grooved lineations, the 'topset' micas displace the 'foreset' micas rather than merging with them.

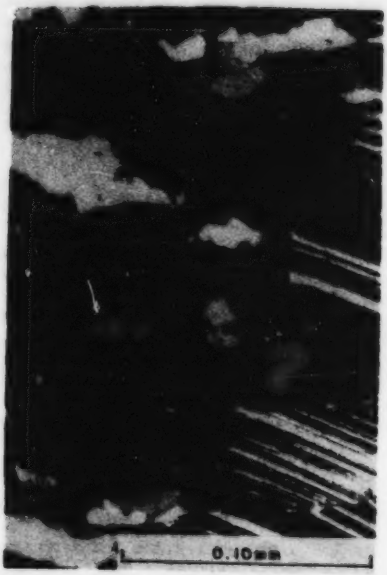

Figure 28. Serrated margin of fibrous quartz veinlet within calcite platelets. Crossed nicols.

Figure 29. Subvertical inclusion bands in a quartz veinlet in a laminated, syn-D_3 vein. The inclusion bands (see arrow) are composed of fragments of calcite. The margins of the quartz vienlet are out of the field of view but lie parallel to the short axis of the photomicrograph. Crossed nicols.

(2) Some of the highly altered rock inclusions that appear intercalated with the platelets in the laminated veins seem to have offset margins (Fig. 31). The displacement or offset is seen along the boundaries between the platelets. Platelet-parallel slip surfaces are present within the inclusions as well as within the principal vein. This type of slip must have occurred after the rock fragments were included in the laminated veins.

(3) Subvertical veinlets, which intruded the platelets in the principal syn-D_s veins, are observed to be locally faulted and folded. Small fractures developed in the subhorizontal inclusion bands displace the subvertical veinlets by as much as 0.20 mm. The recrystallized veinlets are also deformed by drag folds spatially related to the faults (Fig. 32).

(4) In places, the e-lamellae calcite twin is bent approaching the surface of the platelet or is displaced across this surface (Fig. 33). Here a broad glide twin is commonly developed, indicating a differential movement along the platelet surface. Low temperature plastic deformation of this type (Schmid, 1983) is aided by the fact that there are few grain boundaries as an obstacle to movement along the platelet surface (cf. Ashby and Verrall, 1978).

Summary of Syn-D_s Veins

(1) Concordant, principal veins displaying lamination or honeycomb structure are considered as syntectonic D_s veins. They show growth textures which developed while the host rocks carried S_s cleavage. Vein growth ceased, however, while this cleavage continued to develop.

(2) The syn-D_s veins illustrate deformation textures which tend to destroy the growth textures. Deformation was largely controlled by the presence and shape of the platelets so that slip occurred parallel to the lamination.

(3) The inclusion bands in the syn-D_s veins are extremely thin and laterally extensive. They represent either slivers of host rock from the wall of the vein or occluded overgrowths on grains in the vein wall (cf. Cox and Etheridge, 1983). A series of these inclusion bands all parallel to the vein margin suggest that fractures formed repetitively at the vein wall. The material, now represented by each platelet, presumably filled the fracture after it opened. Early cracks (i.e. the platelet-inclusion band boundary) must have been sealed by solid phases before fracturing recurred. New material was added antitaxially at the vein margin as the fracture opened wider and wider. Younger sealants grew in optical continuity with older sealants. This process of repetitive 'cracking and sealing' has been described by Durney and Ramsay (1973) and Ramsay (1980a). Henderson (1983) indicated that some of the principal veins in the Sheet Harbour-Ecum Secum area formed in this way.

(4) Inclusion bands and inclusion trails are present in the subvertical veinlets in the laminated principal veins and in the subvertical side veins in the country rock. This suggests that 'crack-seal' may have also been operative here. In any case, such textures are clearly not of geopetal origin. The regular geometry of all the syn-D_s, subvertical

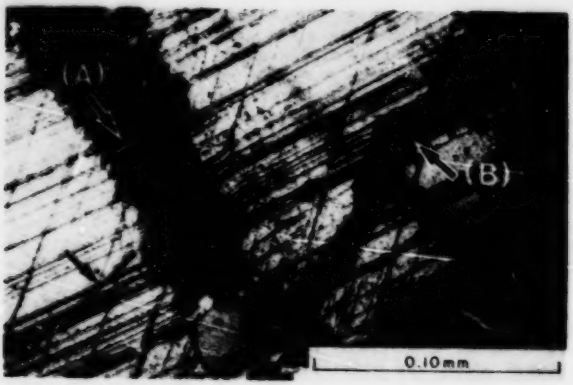

Figure 30. Inclusion trails defined by calcite grains (arrow A) in a subvertical quartz veinlet. The long axes of the calcite grains lie parallel to the surface of the calcite platelets (arrow B) in a laminated, syn-D_8 vein. Crossed nicols.

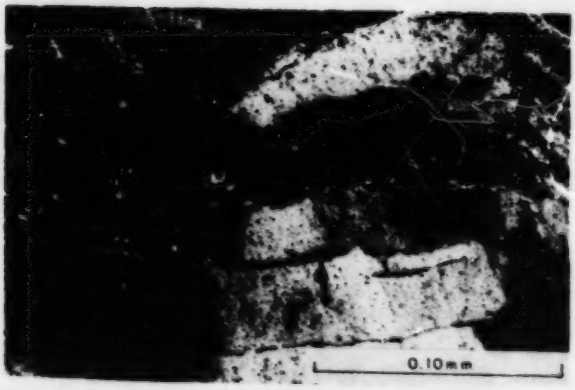

Figure 31. Displacement surfaces, within micaceous bands at platelet boundaries, (see arrow) pass through included rock fragments. Crossed nicols.

Figure 32. Recrystallized veinlets deformed by open folds below a displacement surface (see arrow) parallel to the platelets and inclusion bands in a laminated, syn-D_s vein. Crossed nicols.

Figure 33. An e-lamellae (0112) twin (arrow A) in a calcite platelet is displaced along a (0001) glide twin (arrow B). Crossed nicols.

veinlets indicates that steep fracture patterns existed in flat strata prior to any folding. The steep fracture sets were confined to the environs of what eventually evolved into the principal, syn-D_s veins. Later in the regional deformation, vertical fractures became increasingly important and extended throughout the entire Meguma succession.

MODELS FOR THE ORIGIN OF SYNTECTONIC D_s VEINS

Buckled, internally laminated, lineated veins are common in slate belts. The veins typically lie subparallel to the bedding planes and are folded with the host strata. Such veins have been generally reported to have formed by tectonic movements directly related to the folding process, e.g., flexural slip. Syn-D_s veins, however, can be traced continuously around paired, second and third order F_s anticlines and synclines. Similar relationships between folds and laminated veins have been described from the Stirling Range of southwestern Australia by Boulter (1979) and from the Welsch Slate Belt of Wales by Nicholson (1978). Their historical 'saddle reef' interpretation has been considered suspect because the Meguma veins are not restricted to dilation zones in anticlinal hinges (e.g. Graves and Zentilli, 1982 and Henderson, 1983).

In southwestern Guysborough County during regional D_s deformation and greenschist facies metamorphism, brittle and ductile structures developed synchronously. Synmetamorphic fractures produced at the depths of approximately 10 km (cf. Graves and Zentilli, 1982) are probably hydraulic tensile or shear fractures (cf. Secor, 1965; Sibson, 1981 and Beach 1980). The growth of fibres and platelets in the syn-D_s veins records the dilational or extensional strain during the D_s deformation, whereas S_s cleavage and F_s folds provide evidence of the D_s compressional strain. One set of concordant, principal veins dilated by repeatedly failing along an initial fracture surface rather than producing new vein-filled fractures. There is a notable absence of crosscutting syn-D_s veins within individual beds.

Single crystal platelets with enclosed host rock inclusions record periods of continuous, undisturbed crystallization. The platelets or sealants binding the fracture presumably crystallized in host strata that were once overpressured (Sibson et al., 1975 and Graves and Zentilli, 1982), and already shortened and cleaved. Each time the pressure of the fluid exceeded the shear or tensile strength of the local host rocks, a new 'crack' was formed and strain energy was released seismically (cf. Graves and Zentilli, 1982). Fibrous, dendritic, vermicular growths of penninite 'poikilitically' enclosed in the single crystal platelets (Fig. 34a and b) may represent material precipitated during hydraulic fracturing.

Any model for the origin of the principal syn-D_s veins must explain how the vertical veinlets and the horizontal platelets in the honeycomb structure extended and grew while the host strata were being flattened and cleaved by S_s. Optically continuous single crystals 'seal' both the horizontal and the vertical 'cracks' and include the S_s cleavage. If these 'cracks' are tensile, then the D_s stress ellipsoid must have rotated through 90° on at least two axes while the single crystals precipitated from the mineralizing fluid. Two models are presented to explain these phenomena. Model 1 involves rotating the D_s stress ellipsoid and Model 2 does not.

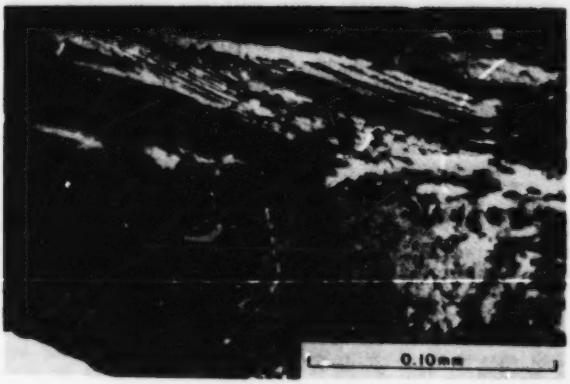

Figure 34a. Dendritic chlorite enclosed 'poikilitically' in a single crystal of quartz. The latter comprises a platelet in a laminated, quartz-carbonate vein. Crossed nicols.

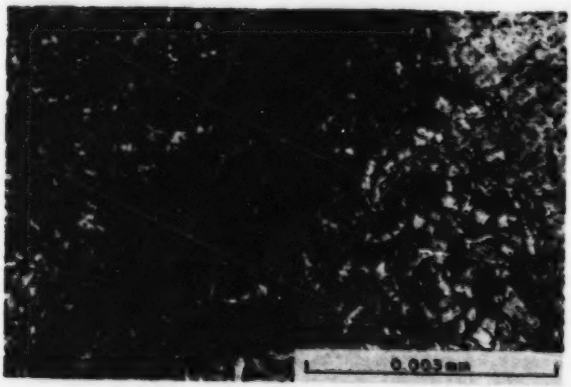

Figure 34b. Vermicular, fibrous growths of chlorite set in optically continuous quartz. Crossed nicols.

Model 1: Burial with Incipient Layer-parallel Shortening

Syntectonic, vertical, veinlet-filled, extensional fractures have been reported to have formed in many localities. Those in the Delamerian fold belt of South Australia (Winsor, 1979), for example, are thought to have occurred during diagenesis when the maximum principal stress was vertical and due to the load of the overburden. There the intermediate and minimum principal stresses were horizontal in the plane of the strata.

In the Meguma Group of southwestern Guysborough County, compaction due to burial in the sedimentary basin could have theoretically produced greenschist facies phyllosilicates defining a fabric parallel to bedding. Such loading could also form vertical, veinlet-filled fractures which opened to include the compaction fabric in directions perpendicular to the maximum principal stress (Fig. 35). The least compressive principal stress would rotate in the horizontal host strata about the vertical axis of maximum principal stress or alternatively, extension could occur equally along both axes contained in the strata. In doing so, two sets of vertical tensile fractures form and intersect to give the observed 'rhomba' in the honeycomb structure (Fig. 6). However, this stress field orientation cannot produce the horizontal fractures sealed by the platelets. To do this, the maximum principal stress must be applied parallel to the flat strata with the minimum principal stress vertical (Fig. 35). This is an incipient layer-parallel shortening situation (Graves and Zentilli, 1982) in which bedding-parallel foliations cannot develop. Overlapping age relationships between vertically extending platelets and horizontally extending veinlets mean that the axis of maximum principal stress or the direction of greatest extensional strain or both must repeatedly rotate from the vertical to the horizontal and vice versa. A steep cleavage apparently did not develop as the platelets grew. In this model the horizontal foliation in the platelets and in the platelet-parallel inclusion bands would have to be incorporated as 'xenoliths' and not as syntectonic trails.

Model 2: Layer-parallel Shear

Compressional strains of D_2 age produced the S_2 cleavage and the F_2 folds in southwestern Guysborough County. The writer has recently modelled these features in terms of a regional D_2 shear parallel to the horizontal strata of the Meguma Group (O' Brien, 1983a, b). The interbedded sandstones and shales behave mechanically as a multilayer and are deformed by differential slip apparently without detachment. An analogy is the shearing of a deck of playing cards on a table top. The horizontal bedding planes are the principal planes of shear and the strata occur within what are essentially flat-lying shear zones.

In this model the S_2 foliation is held to be a hard-rock cleavage formed during regional shear. It is thought not to be a compaction fabric because (1) it generally cuts through the flat-lying beds at a low angle, (2) it is axial planar to minor F_2 folds affecting veins and altered host rocks, and (3) it is found parallel to bedding only in the relatively incompetent beds. Since S_2 occurs as inclusion trails in the principal veins, it is postulated that vein-filled fractures also formed

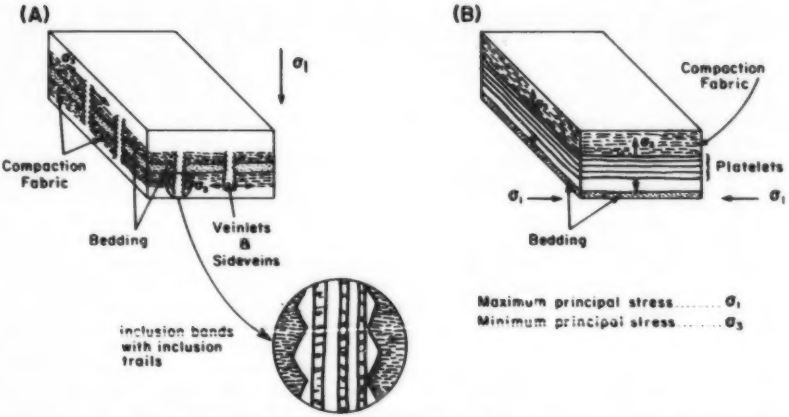

Figure 35. Models depicting the stress orientations for tensile fractures formed during compaction and diagenesis. (A) portrays the concomitant development of vertical veinlets and a horizontal compaction fabric in flat strata affected by a vertical maximum principal stress; (B) shows the opening of the horizontal platelets in flat strata carrying a bedding-parallel compaction fabric. Here the maximum principal stress is applied in the horizontal plane.

during layer-parallel shear, their dilation being some measure of the D_s extensional strain. Boulter (1979), Nicholson (1966), and Morris and Barron (1968) have previously described laminated veins and offshoots similar to the syn-D_s veins that probably originated by some form of shear along bedding. This tectonic movement was thought to have occurred prior to the development of the upright periclines about which the veins eventually became disposed.

During layer-parallel shear the maximum principal stress was neither parallel nor perpendicular to the horizontal strata. Instead, it was inclined at some acute angle to the bedding planes or the shear planes (Fig. 36). As a result, there was a finite shear stress active across the beds in the shear zones. Hydraulic tensile fractures in the form of primary or secondary D_s tension gashes could theoretically be expected (Ramsay and Graham, 1970; Beach, 1975, 1977; Kerrich and Allison, 1978). They would form dipping at approximately 45° in the flat-lying strata (Fig. 36A). Veins such as these are not observed in southwestern Guysborough County. In fact, a 5°-15° angular discordance between bedding and the principal, syn-D_s veins is a notable, probably original, feature. However, certain types of hydraulic shear fractures can develop in the layer-parallel shear model at a low angle to bedding. Because the shear fractures are opened and filled, there must also be a component of normal stress active across the 'crack' (i.e. an oblique extension). Hancock (1972) suggested that fractures such as these are hybrid, belonging to the transition between compressional shear fractures and extensional tensile fractures.

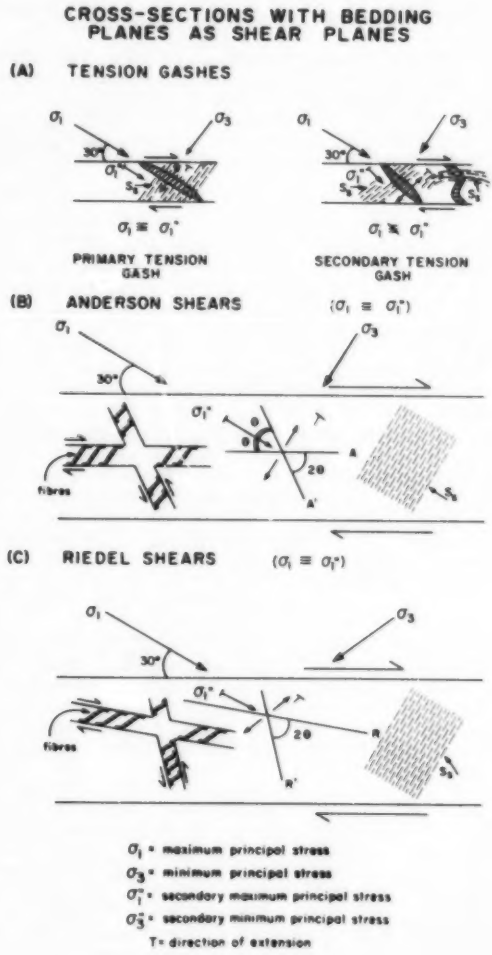

Figure 36. Models depicting the stress orientations for shear and tensile fractures formed during D_8 layer-parallel shear. (A), (B) and (C) are cross-sections of a horizontal bed with the bedding planes acting as shear planes. The maximum principal stress is drawn with a constant orientation with respect to bedding and the principal shear planes in (A), (B) and (C); see text for discussion.

Shear fractures in ductile-brittle shear zones are commonly produced in conjugate sets. They can be either Anderson-type shear fractures (cf. Ramsay, 1980b) or Riedel-type shear fractures (cf. Tchalenko, 1970). In the case of Anderson-type shear fractures the maximum principal stress is the acute bisectrix of the angle (2θ) between the conjugate sets (Fig. 36B). Where such fractures are symmetrically disposed about the maximum principal stress acting on the flat-lying shear zones, one conjugate set (A) lies subparallel to the bedding planes or shear planes and the other set (A') is subperpendicular to them (Beach, 1975 and Rickard and Rixon, 1983). The Anderson-type shear fractures are extended parallel to the minimum principal stress and become vein-filled. In contrast, conjugate Riedel shears occur asymmetrically about the maximum principal stress. The principal R-shear forms at 5°-15° to the principal shear plane and its conjugate pair, the R'-shear, at 70°-85° (Fig. 36C). If the principal syn-D_s veins occupy R-shears in flat strata, then they were produced subparallel to bedding. If conjugate R'-shears are present as veinlets, they would develop with a steep dip through the host strata and the principal veins. Once formed, the Riedel shears would open parallel to the most tensile stress within the shear zone. Alternatively, the D_s vein-filled fractures may be hybrid, partly shear and partly tensile. If so, they would originate as fractures dipping between 15°-40° in the horizontal strata (Hancock, 1972). Such veins have been reported to have formed in secondary stress fields governed by local Riedel shear systems (Rickard and Rixon, 1983).

If the layer-parallel shear model is correct, then the principal, syn-D_s veins occupy dilatant shear fractures. The low angle discordancy between vein and host strata is a consequence of repeated and preferential hydrofracturing along one of the conjugate sets. The subhorizontal platelets would have 'sealed' the conjugate fractures subparallel to bedding. Subvertical veinlets and side veins may 'seal' the opposing set of conjugate fractures. Gently dipping dilatant shear fractures may be connected with their steeply dipping, conjugate pairs by single, optically continuous crystals. In this model, the mineralizing fluid can pass contemporaneously through open fractures and the axes of the D_s stress ellipsoid are not required to rotate from vertical to horizontal positions as the platelets and veinlets evolve. The S_s foliation formed concomitantly with the veins as a gently dipping, hard-rock cleavage normal to the maximum principal stress acting on the flat-lying shear zones. With progressive D_s deformation, the S_s cleavage and the principal veins come to lie closer to the bedding planes and the veins eventually become folded by F_s folds.

ACKNOWLEDGMENTS

I thank P. K. Smith, J. R. Henderson, S. J. Haynes, A. K. Chatterjee and J. D. Keppie for discussion and advice. C. K. Mawer reviewed the manuscript and offered many useful suggestions. This is a contribution to the Canada - Nova Scotia Co-operative Mineral Program 1981-84, mainly funded by the Province of Nova Scotia.

REFERENCES

Ashby, M. F. and Verrall, R. A.
1978: Micromechanisms of flow and fracture and their relevance to the rheology of the upper mantle; *in* Philosophical Transactions of the Royal Society of London, A288, p. 59-95.

Beach, A.
1975: The geometry of en échelon vein arrays; Tectonophysics, v. 28, p. 245-263.

1977: Vein arrays, hydraulic fractures and pressure solution structures in a deformed flysch sequence, S. W. England; Tectonophysics, v. 40, p. 201-225.

1980: Numerical models of hydraulic fracturing and the interpretation of syntectonic veins; Journal of Structural Geology, v. 20, no. 4, p. 425-438.

Boulter, C. A.
1979: On the production of two inclined cleavages during a single folding event, Stirling Range, S. W. Australia; Journal of Structural Geology, v. 1, no. 3, p. 207-219.

Cox, S. S. and Etheridge, M. A.
1983: Crack-seal fibre growth mechanisms and their significance in the development of oriented layer silicate microstructure; Tectonophysics, v. 92, p. 147-170.

Durney, D. W. and Ramsay, J. G.
1973: Incremental strains measured by syntectonic crystal growths; *in* Gravity and Tectonics, eds. K. DeJong, and R. Scholten; Wiley Interscience, New York, p. 67-96.

Graves, M. C. and Zentilli, M.
1982: A review of the geology of gold in Nova Scotia; *in* Geology of Canadian Gold Deposits, eds. R. W. Hodder and W. Petruk; Canadian Institute of Mining and Metallurgy, Special Volume 24, p. 233-242.

Hancock, P. L.
1972: The analysis of en échelon veins; Geological Magazine, 109, p. 269-276.

Haynes, S. J.
1983: Typomorphism of turbidite-hosted auriferous quartz veins, southern Guysborough County; *in* Mines and Minerals Branch, Report of Activities, 1982; Nova Scotia Department of Mines and Energy, Report 83-1, p. 183-225.

Henderson, J. R.
1983: Analysis of structure as a factor controlling gold mineralization in Nova Scotia; *in* Current Research, Part B; Geological Survey of Canada, Paper 83-1B, p. 13-21.

Kerrich, R. and Allison, I.
1978: Vein geometry and hydrostatics during Yellowknife mineralization; Canadian Journal of Earth Sciences, v. 15, p. 1653-1660.

Nicholson, R.
1966: The problem of origin, deformation and recrystallization of calcite-quartz bodies; Geological Journal, v. 5, pt. 1, p. 117-126.

1978: Folding and pressure solution in a laminated calcite-quartz vein from the Silurian slates of the Llangollen region of North Wales; Geological Magazine, v. 115, pt. 1, p. 47-54.

Norris, D. K. and Barron, K.
1968: Structural analysis of features on natural and artificial faults; *in* Conference on Research in Tectonics, eds. A. J. Baer and D. K. Norris; Geological Survey of Canada, Paper 68-52, p. 136-174.

O'Brien, B. H.
1983a: The structure of the Meguma Group between Gegogan Harbour and Country Harbour, Guysborough County; *in* Mines and Minerals Branch, Report of Activities, 1982; Nova Scotia Department of Mines and Energy, Report 83-1, p. 145-181.

1983b: Slate belt tectonics in the Bickerton Barrens, Nova Scotia: horizontal extension and simple shear within the Meguma Basin; (Abstract) Maritime Sediments and Atlantic Geology, v. 19, p. 93.

Ramsay, J. G.
1980a: The crack-seal mechanism of rock deformation; Nature, v. 284, p. 135-139.

1980b: Shear zone geometry: a review; Journal of Structural Geology, v. 2, no. 1-2, p. 83-99.

Ramsay, J. G. and Graham, R. H.
1970: Strain variation in shear belts; Canadian Journal of Earth Sciences, v. 7, p. 786-813.

Rickard, M. J. and Rixon, L. K.
1983: Stress configurations in conjugate quartz-vein arrays; Journal of Structural Geology, v. 5, no. 6, p. 573-578.

Schmid, S. M.
1983: Microfabric studies as indicators of deformation mechanisms and flow laws operative in mountain building; *in* Mountain Building Processes, ed. K. J. Hsu; New York Academic Press, 1983.

Secor, D. T.
1965: Role of fluid pressure in jointing; American Journal of Science, v. 263, p. 633-646.

Sibson, R. H.
1981: Controls on low-stress hydro-fracture dilatancy in thrust, wrench and normal fault terrains; Nature, v. 289, p. 665-667.

Sibson, R. H., Moore, J. M. and Rankin, A. H.
1975: Seismic pumping - a hydrothermal fluid transport mechanism; Journal of the Geological Society of London, v. 131, p. 653-659.

Smith, P. K.
1983: Geology of the Cochrane Hill gold deposits; *in* Mines and Minerals Branch, Report of Activities, 1982; Nova Scotia Department of Mines and Energy, Report 83-1, p. 225-256.

Tchalenko, J. S.
1970: Similarities between shear zones of different magnitudes; Bulletin Geological Society America, v. 81, p. 1625-40.

Winsor, C. N.
1979: The correlation of fracture directions with sediments anisotrophy in folded rock of the Delamerian fold belt at Port Germein gorge, South Australia; Journal of Structural Geology, v. 1, no. 3, p. 245-254.